An improved numerical analysis of flux distributions in anisotropic materials

Takayoshi Nakata
Okayama University

K. Fujiwara
Okayama University

N. Takahashi
Okayama University

Masanori Nakano
Okayama University

N. Okamoto
Okayama University

An Improved Numerical Analysis of Flux Distributions in Anisotropic Materials

T.Nakata, K.Fujiwara, N.Takahashi, M.Nakano and N.Okamoto
Department of Electrical and Electronic Engineering,
Okayama University, Okayama 700, Japan

Abstract **– The method for analyzing flux distributions in transformer cores made of grain-oriented silicon steel is improved in order to reduce error in calculation due to anisotropy in magnetic materials. A model to verify the improved method is proposed, and the calculated results are compared with measured ones.**

I. Introduction

The flux distributions in transformer cores made of grain-oriented silicon steel have been analyzed using only two B-H curves in both rolling and transverse directions[1]. However, the magnetic characteristic along the magnetic hard axis cannot be represented exactly by this method [2-4].

In this paper, firstly, problems of the conventional modelling methods are discussed. Secondly, improvement of the method of analysis is described. Finally, the verification of the software for anisotropic analysis is proposed.

II. Problems of Conventional Methods

The magnetic field strengths, H_x, H_y and H_z, in the x-, y- and z-directions are functions of flux densities, B_x, B_y and B_z, in respective directions as shown in (1) [3-5].

$$\left.\begin{aligned} H_x &= f_x\ (B_x, B_y, B_z) \\ H_y &= f_y\ (B_x, B_y, B_z) \\ H_z &= f_z\ (B_x, B_y, B_z) \end{aligned}\right\} \qquad (1)$$

In the conventional method [1], for example, H_x is assumed to be a function of only B_x, then, (2) has been used instead of (1).

$$\left.\begin{aligned} H_x &= f_x{}^*\ (B_x) \\ H_y &= f_y{}^*\ (B_y) \\ H_z &= f_z{}^*\ (B_z) \end{aligned}\right\} \qquad (2)$$

where f and f^* denote functions.

For simplicity, let us explain in 2-D (only x- and y-components). We define that the x-direction is the rolling direction (R.D.), namely the magnetic easy axis, and the y-direction is the transverse direction (T.D.). Fig.1 shows the loci of $\boldsymbol{B}$ for constant $|\boldsymbol{H}|$. Fig.1(a) shows the measured curves and Fig.1(b) shows the curves calculated using (2). The distance between the origin and a point on the locus corresponds to $|\boldsymbol{B}|$. When the distance is long, the permeability is large, because $|\boldsymbol{H}|$ is constant on the locus. Therefore, the magnetic easy axis estimated from the conventional modelling method shown in Fig.1(b) is completely different from the actual easy axis, which coincides with the rolling direction (x-direction). Fig.1 denotes that the permeability estimated from (2) is higher than that for the magnetic easiest axis at the high flux density region. This discrepancy is due to the assumption in (2).

Fig.2 is an example which denotes the functions of (1) for the 2-D case. The B-H curves are measured [3] for 0.3mm thick highly grain-oriented silicon steel (AISI : M-0H). In the

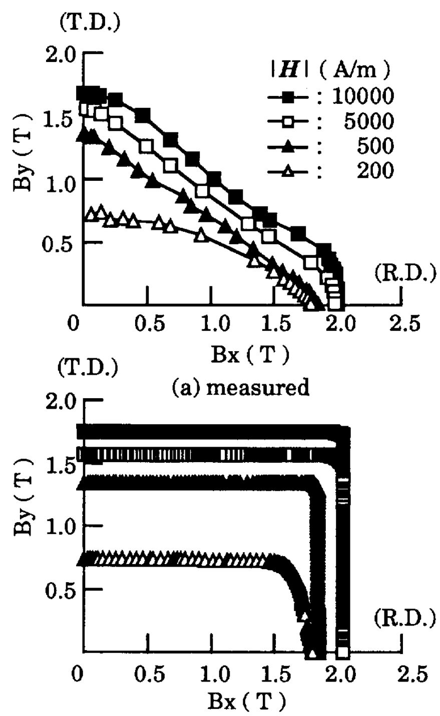

(b) conventional (approximation using Eq.(2))

Fig.1 Loci of $\boldsymbol{B}$ for constant $|\boldsymbol{H}|$ (AISI : M-0H, 0.3mm).

Manuscript received November 1, 1993.

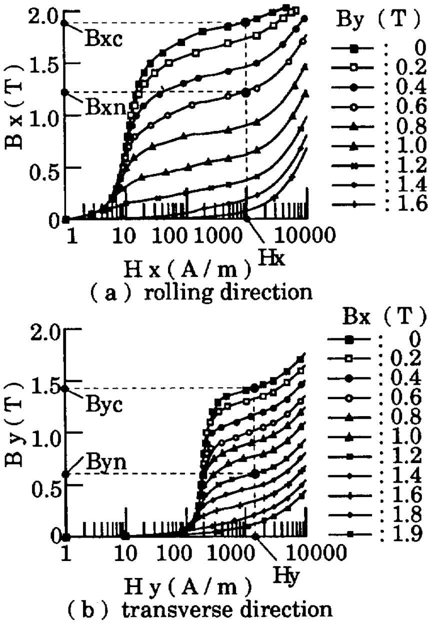

Fig.2 B-H curves (AISI : M-0H, 0.3mm).

conventional method[1], only two B-H curves, namely, B_x-H_x curve for B_y=0 and B_y-H_y curve for B_x=0 are used. If $\boldsymbol{H}$ vector is specified, the x- and y-components, B_{xc} and B_{yc}, obtained using the conventional approximation method (2) is much higher than those, B_{xn} and B_{yn}, obtained using (1) as shown in Fig.2. Therefore, the flux density $|\boldsymbol{Bc}|$ which is denoted by (3) is overestimated in the analysis using the conventional method.

$$|\boldsymbol{B_c}| = \sqrt{B_{xc}^2+B_{yc}^2} \quad > |\boldsymbol{B_n}| = \sqrt{B_{xn}^2+B_{yn}^2} \quad (3)$$

Similarly, the magnetizing current is underestimated, when the flux which is interlinked with the anisotropic material is specified.

Fig.3 shows the relationship between θ_B and θ_H. θ_B and θ_H are the angles of $\boldsymbol{B}$ and $\boldsymbol{H}$ vectors from the rolling direction. It is obvious that there is a large discrepancy between the actual phenomena (Fig.3(a)) and the conventional modelling (Fig.3(b)). Namely, in Fig.3(a), θ_B is larger than θ_H, only when $|\boldsymbol{H}|$ is large and $\theta_B \approx 90$deg. In Fig.3(b), θ_B is larger than θ_H, only when $|\boldsymbol{H}|$ is large and θ_B is small.

In order to improve the above-mentioned discrepancy, an elliptic model has been proposed[6-8]. The locus of $\boldsymbol{B}$ shown in Fig.1(a) is tried to be approximated by an elliptic curve as shown in Fig.4. Although the curves at low flux density region are similar to those in Fig.1(a), B_x-H_x and B_y-H_y curves converted from the elliptic curves which are shown in Fig.5 are much different from the measured curves shown in Fig.2 which are

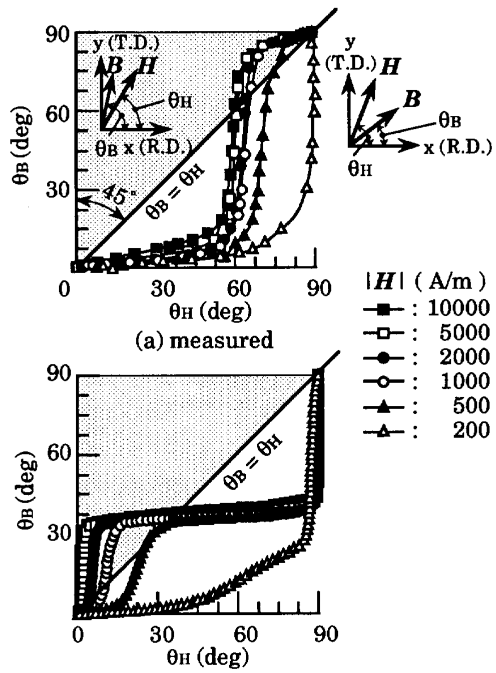

(b) conventional (approximation using Eq.(2))

Fig.3 θB-θH curves for constant |*H*| (AISI : M-0H, 0.3mm).

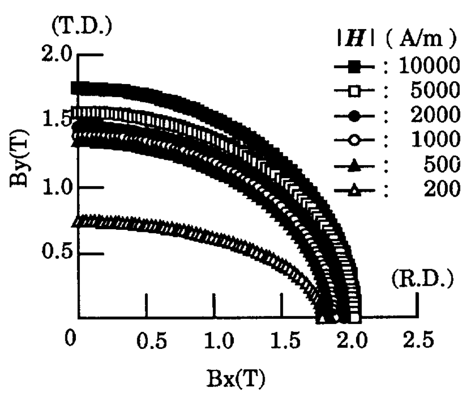

Fig.4 Elliptic model (approximation using Eq.(4)) (AISI : M-0H, 0.3mm).

denoted by dotted lines, because the permeabilities, μ_x and μ_y, are constant on the elliptic curve for the constant $|\boldsymbol{H}|$ as shown in (4).

$$\left(\frac{B_x}{\mu_x}\right)^2 + \left(\frac{B_y}{\mu_y}\right)^2 = H^2 \qquad (4)$$

III. Improved Method of Analysis

When the anisotropic magnetic field is analyzed using the B-H curves shown in Fig.2, the coefficient, $\partial G_i^{(k)}/\partial A_j^{(k)}$, at the k-th nonlinear

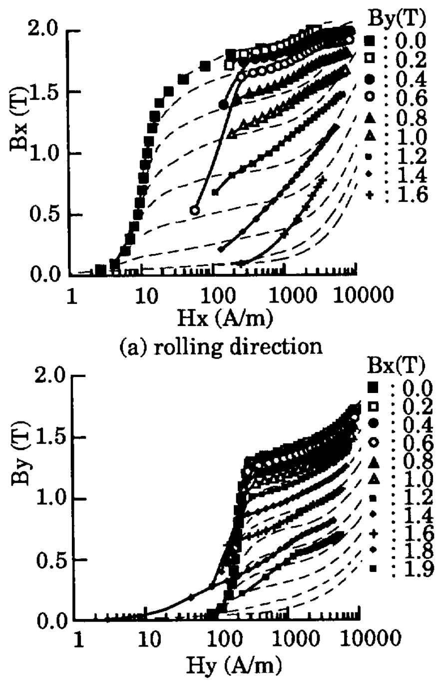

(a) rolling direction

(b) transverse direction

Fig.5 B-H curves for elliptic model (AISI : M-0H, 0.3mm).

iteration in Newton-Raphson method can be represented by the following function:

$$\frac{\partial G_i^{(k)}}{\partial A_j^{(k)}} = g\left(\frac{\partial H_x^{(k)}}{\partial B_x^{(k)}}, \frac{\partial H_x^{(k)}}{\partial B_y^{(k)}}, \frac{\partial H_y^{(k)}}{\partial B_x^{(k)}}, \frac{\partial H_y^{(k)}}{\partial B_y^{(k)}}\right) \quad (5)$$

where g denotes a function. G_i and A_j are the residual at a node i and the magnetic vector potential at a node j respectively. The coefficient matrix is unsymmetric due to $\partial H_x/\partial B_y$ and $\partial H_y/\partial B_x$ (In the conventional methods, it is symmetric due to the assumption (2)).

In order to avoid solving unsymmetrical linear equations, the calculation procedure is improved as shown in Fig.6. Step① : Let us consider only one B-H curve in Figs.2(a) and (b) respectively in an element during the Newton-Raphson iteration (N.R.)[9,10]. Therefore, in step①, $\partial H_x/\partial B_y$ and $\partial H_y/\partial B_x$ in (5) can be assumed to be zero. Step② : When B_x, H_x, B_y and H_y are determined at the end of N.R. iteration, the new B-H curve in Fig.2(a) is chosen from the new $B_{y(l)}$ at the l-th iteration and that in Fig.2(b) is chosen from the new $B_{x(l)}$. If there is no desired B-H curve in Fig.2, the B-H curve required is calculated by interpolation[11]. When the difference between the new flux density $\boldsymbol{B}_{(l+1)}$ and the former one $\boldsymbol{B}_{(l)}$ is less than 0.01T,

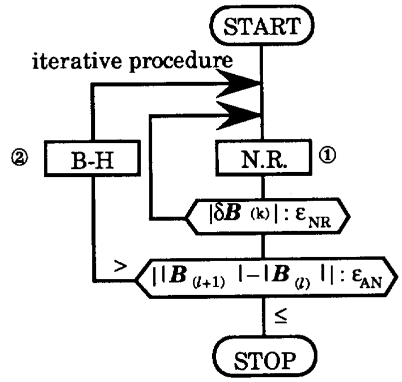

ε_{NR}, ε_{AN} : convergence criterions

Fig.6 Flow chart.

the iterative process is terminated.

The improved method mentioned above has the following advantages:

(i) The software can be made by the minor change of the conventional one.
(ii) As the coefficient matrix is symmetric, the ICCG method[12] can be applied to solve the linear equations.

The disadvantages are as follows:

(i) It cannot be guaranteed to get the convergence.
(ii) It takes a long CPU time due to the iterations for changing B-H curves.

IV. Verification of Software

A. Verification model

Fig.7 shows a single-phase transformer core made of the same material as that in Fig.2. The shape is chosen so that the result calculated using the conventional method is very much different from that using the improved method. The core is laminated by 70 sheets(0.3×180×400mm). A rectangular window(40×220mm) is bored in each sheet.

B. FEM analysis and experimental results

The magnetic vector potential $\boldsymbol{A}$ is used in the 2-D finite element analysis. Fig.8 shows the flux distributions at practical flux density (B_{leg}=1.7T) and at low flux density (B_{leg}=0.5T). B_{leg} is the average flux density in the leg.

Fig.9 shows the distributions of the absolute value $|\boldsymbol{B}|$ and the angle θ_B of the flux density deviated from the rolling direction along the line α-β in Fig.7. The flux densities can be measured using a search coil which is wound through 0.6mm holes drilled in the 70 laminations as shown in

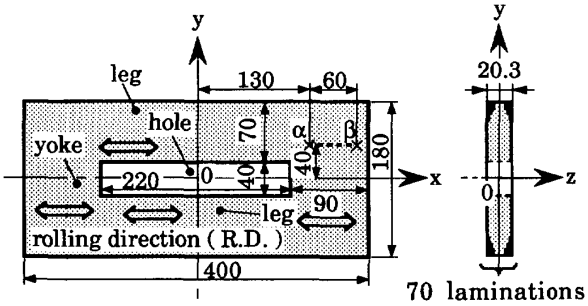

Fig.7 Verification model.

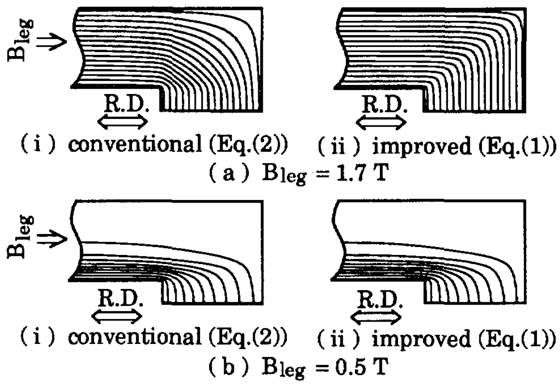

Fig.8 Flux distributions (AISI : M-0H, 0.3mm).

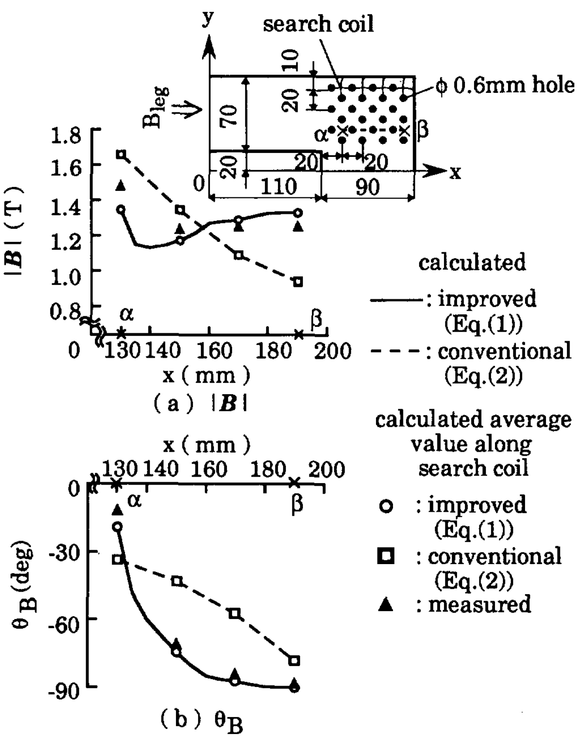

Fig.9 Comparison between calculated and experimental results (B_{leg}= 1.7 T).

Fig.9. Fig.9 suggests that the results obtained by the improved method are nearer to the measured ones than those calculated by the conventional method.

V. Conclusions

The problems of conventional modelling methods for anisotropic B-H curves are examined. An improved method is introduced, and a verification model is proposed. The results obtained can be summarized as follows:

(1) B_x-H_x and B_y-H_y curves of the conventional methods are much different from the actual curves.

(2) Results calculated using the improved method are in good agreement with measured results.

References

[1] T.Nakata, Y.Ishihara, K.Yamada and A.Sasano, "Non-linear analysis of rotating-flux in the T-joint of a three-phase, three limbed transformer core", *Proceedings of the Soft Magnetic Materials 2 Conference*, pp.57-62, 1975.

[2] T.Nakata, K.Fujiwara and M.Sakaguchi, "Non-linear 3-D magnetic field analysis of corner joints of a transformer core using the finite element method", *Papers of the Joint Technical Meeting on Static Apparatus and Rotating Machines of IEEJ*, nos.SA-87-33 and RM-87-70, pp.149-158, 1987.

[3] T.Nakata, N.Takahashi, K.Fujiwara and M.Nakano, "Measurement of magnetic characteristics along arbitrary directions of grain-oriented silicon steel up to high flux density", *IEEE Trans. Magnetics*, vol.MAG-29, no.5, November 1993 (to be published).

[4] T.Nakata, N.Takahashi, K.Fujiwara and M.Nakano, "Numerical analysis of flux distributions in cores made of anisotropic materials (invited)", *Journal of Magnetism and Magnetic Materials*, vol.113, 1994 (to be published).

[5] M.Kasper and A.Kost, "Finite element field analysis in ferromagnetic materials under consideration of anisotropy and saturation", *Electrosoft*, vol.1, no.3, pp.205-213, 1990.

[6] A. di Napoli and R.Paggi, "A model of anisotropic grain-oriented steel", *IEEE Trans. Magnetics*, vol.19, no.4, pp.1557-1561, July 1983.

[7] D.Shen, J.C.Sabonnadiere, G.Meunier, J.L.Coulomb and M.Sacotte, "3D anisotropic magnetic field calculation in transformer joints", *ibid.*, vol.23, no.5, pp.3783-3785, September 1987.

[8] P.P.Silvester and R.L.Ferrari, *Finite Elements for Electrical Engineers*, 2nd ed., Cambridge University Press 1990.

[9] T.Nakata, N.Takahashi, K.Fujiwara, N.Okamoto and K.Muramatsu, "Improvements of convergence characteristics of Newton-Raphson method for nonlinear magnetic field analysis", *IEEE Trans. Magnetics*, vol.MAG-28, no.2, pp.1048-1051, March 1992.

[10] K.Fujiwara, T.Nakata, N.Okamoto and K.Muramatsu, "Method for determining relaxation factor for modified Newton-Raphson method", *ibid.*, vol.MAG-29, no.2, pp.1962-1965, March 1993.

[11] H.Haas and F.Schmoellebeck, "Approximation of nonlinear anisotropic magnetization characteristics", *ibid.*, vol.MAG-28, no.2, pp.1255-1258, March 1992.

[12] K.Fujiwara, T.Nakata and H.Fusayasu, "Acceleration of convergence characteristic of the ICCG method", *ibid.*, vol.MAG-29, no.2, pp.1958-1961, March 1993.